Kovove Mater. 55 2017 97–106
DOI: 10.4149/km_2017_2_97

Microstructure examination of functionally graded NiTi/NiAl/Ni_3Al intermetallic compound produced by self-propagating high-temperature synthesis

M. Kilic[1], I. Kirik[2], M. Okumus[2]*

[1] *Batman University, Faculty of Technology, Manufacturing Engineering, 72000 Batman, Turkey*
[2] *Batman University, Faculty of Architecture and Engineering, Department of Metallurgical and Materials Engineering, 72000 Batman, Turkey*

Received 29 December 2015, received in revised form 17 May 2016, accepted 18 May 2016

Abstract

In this study, functionally graded Ni_3Al/NiAl/NiTi material was produced by Ni-Ti-Al powders at 150 MPa compaction pressure and at different pre-heating temperatures (200, 300, and 400 °C) using self-propagating high-temperature synthesis (SHS) method. This material was ignited with the help of external heat, after it was subjected to pre-heating under argon atmosphere, following the stages of atomic weighing, mixing, and pressing of powders under a defined compaction pressure respectively before the ignition. Microstructure examinations of the functionally graded material (FGM) being successfully synthesized after ignition, were performed by using an optical microscope, SEM (scanning electron microscope), and EDS (energy dispersive spectroscopy) methods. It was observed that owing to the exothermic reaction occurring as a result of self-propagating high-temperature synthesis, the cohesion of powders consisting of compacted 3 different layers occurred, combustion pits formed in samples after ignition, and intermediate phases with primary phases and dendritic branches were formed at the microstructure analysis.

Key words: functionally graded material (FGM), self-propagating high-temperature synthesis (SHS), microstructure

1. Introduction

Functionally graded materials (FGM) are the new generation engineering materials drawing attention in recent years. The concept of FGM is based on the graded alternation of its composition in order to prevent thermal stresses at a sharp interface developed in the structure and material. FGMs were firstly discovered by scientists in Japan in the 1980s as ultra-light heat-resistant material for space crafts and accepted as a nominee for applications in the solution of the problems which extremely modern technologies face in serious environments [1–5]. These materials having unique properties are an improved class of engineering composites comprising continuous and smoothly varying combination of two or more materials [6, 7]. Because they contain the pure form of each component in FGM, the problem of the balance needed in traditional materials is eliminated in these materials. Thus the properties of both components can be fully used [8]. Production techniques in a wide range, including rapid manufacturing techniques, have been developed.

As the production methods of FGM: magnetic spraying, physical vapor decomposition, dynamic ion mixing, chemical vapor infiltration, and reaction bonding methods along with powder metallurgy (P/M) techniques, plasma spraying techniques, chemical vapor decomposition, self-propagating high-temperature synthesis (SHS), were used. Powder metallurgy techniques used among these methods are mostly used for the production of FGMs consisting of plates (layers) having millimeter thick dimensions due to self-propagation speed, and simplicity and economy of the method [9–11]. SHS method, which is one of the most preferred methods among the powder metallurgy methods, becomes prominent as an advanta-

---

*Corresponding author: tel.: +90 488 217 3501; fax: +90 488 217 3601; e-mail address: mustafa.okumus@batman.edu.tr

Table 1. Characteristics of powders used in the experimental study [24]

Material	Purity degree by weighing (%)	Powder size (mesh)	Melting temperature (℃)	Specific weight (g cm^{-3})	Atomic mass (g mol^{-1})	Boiling temperature (℃)
Nickel	99.5	–325	1453	8.908	58.71	2832
Aluminum	99.5	–325	660.4	2.7	26.9	1081
Titanium	99.5	–325	1680	4.507	47.9	3260

geous method due to lower energy consumption and shorter process times, simple processing equipment, lower cost, and better condition of starting materials [12]. Combustion synthesis has drawn wide attention among different methods due to its characteristics because this method is based on the principle of starting ignition process for some of the previously synthesized elemental compositions, i.e. compacted powder particles by using an external igniter. With starting of ignition, the energy required through compacted sample is possible by propagation of combustion wave occurring through an exothermic reaction started between elemental compositions affordably without any expensive device. FGMs have been successfully used as thermal barrier coating material for turbine blades, shield protection for military applications, fusion energy devices, biomedical, coating for edges of cutting tools, engine parts of automobiles, heat exchangers, fire retardant plates, for manufacturing the components of nuclear reactors [13–17].

In the 1950s and 1960s, NiAl alloys were used as coating materials for thermal components in corrosive environments. Oxidation resistance of NiAl can be considerably developed by alloying with other refractory elements such as yttrium, hafnium, and zirconium [18, 19]. In 2001, Kopit examined the Ni-Al-Ti based metallic compounds produced by SHS method under nitrogen and argon. He stated that nitrogen gas had expanded significantly flame propagation limit because of added heat emitted during the manufacturing the nitride [20]. In 2009, Chen et al. produced the formation of FGM TiB2-Ni/Ni3Al/CrNi alloy by using area active combustion synthesis. As a result of their study, they revealed the practicability of area active combustion synthesis with the assistance of pressure in order to form FGMs rapidly along with a good diffusion between layers [21]. Kumar et al., 2011, conducted studies on intermetallic nickel aluminates (Ni_3Al) to change the current automotive body and determine the suitability of this material. They stated that this alloy would be a good nominee material for automotive bodies due to the increase of hardness value of Ni3Al alloy by hot annealing and at the same time its high strength [22]. Burkes et al., 2006, expressed that production of functionally graded material (FGM) NiTi-TiCx composite was possible by the use of propagating mode (SHS) of a combustion synthesis reaction [23].

As a result of the reviews, the number of studies conducted on the functionally graded Ni_3Al/NiAl/NiTi material which was produced by Ni-Ti-Al powders with the help of the self-propagating high-temperature synthesis method is very limited. Thus, effects of micro and macro structure of functionally graded material consisting of different layers after joining were tried to be determined in this study.

2. Material and method

In this study, powders of nickel, titanium, and aluminum (99.5 % pure Ni, 99.5 % pure Al, and 99.5 % Ti) used in the production of intermetallic FGMs were supplied from Alfa Easer Company. The mean size of powders was commercially supplied as –325 mesh. Table 1 illustrates chemical combinations of these materials.

Before the production process, commercially supplied Ni, Ti, and Al powders and Ni-Al, Ni_3-Al, and Ni-Ti powders prepared by atomic weighing were mixed in different containers for 24 h at 16 rpm in a specially designed rotating container in order to provide a homogeneous mixture. Mixed powders were cold pressed at 150 MPa in a 12 mm diameter cylinder shaped steel powder compaction mold.

A manually controlled ignition unit in dimensions of 40 × 40 × 30 mm^3 was used to provide pre-heating and to perform ignition process for pressed pieces. This apparatus of ignition unit is composed of five major components. These consist of a pre-heating chamber, ignition center, and chamber, fixing piston, temperature adjusting button, and inlet and outlet parts of argon gas. After pressed samples had been annealed at 200, 300, and 400 ℃ pre-heating temperatures in ignition unit, they were ignited in argon gas environment by using SHS method. Figure 1 illustrates the sample obtained after ignition.

3. Results and discussion

3.1. Microstructure examination

It was observed that the synthesizing process was

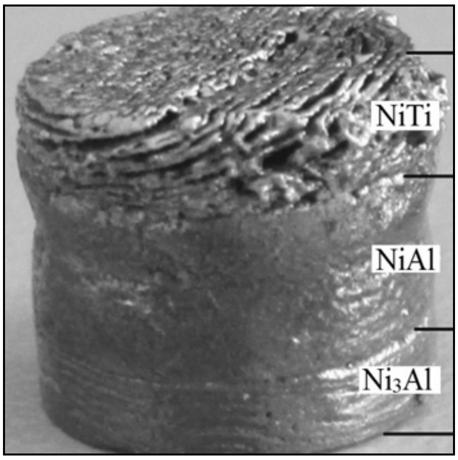

Fig. 1. Macrograph of FGM obtained after ignition.

performed successfully from the macrographs of samples produced after ignition by using 150 MPa pressing pressure and 200, 300, and 400 ℃ of pre-heating temperatures (see Figs. 2a–c). As the macro photographs of the samples were examined, it was observed that integrity of sample was preserved at 200 and 300 ℃ of pre-heating temperatures, NiTi side was totally joined, but combustion halls were formed in the NiAl-Ni_3Al side as well. The main reason for this was associated with more melting because of the high reaction heat occurring during the transformation from NiAl to Ni_3Al. However, it is observed that this integrity was deformed at 400 ℃ of pre-heating temperature, layers tended to separate even not completely rather than formation of combustion hall in NiTi-NiAl zone, the combustion hall did not form in NiAl-Ni_3Al zone, and a proper joining did not occur because of the high pre-heating temperature.

As it is seen in optical microstructure images taken from main materials and interfaces of synthesized sample showed that pores formed out of interfaces at 200 and 300 ℃ of pre-heating temperatures, but pores concentrated at NiAl layer and this situation disappeared in other areas at 400 ℃ of pre-heating temperature (Figs. 3–5). At the same time, the existence of intense dendritic formation in the intersection of NiTi-NiAl was observed from optical microstructure im-

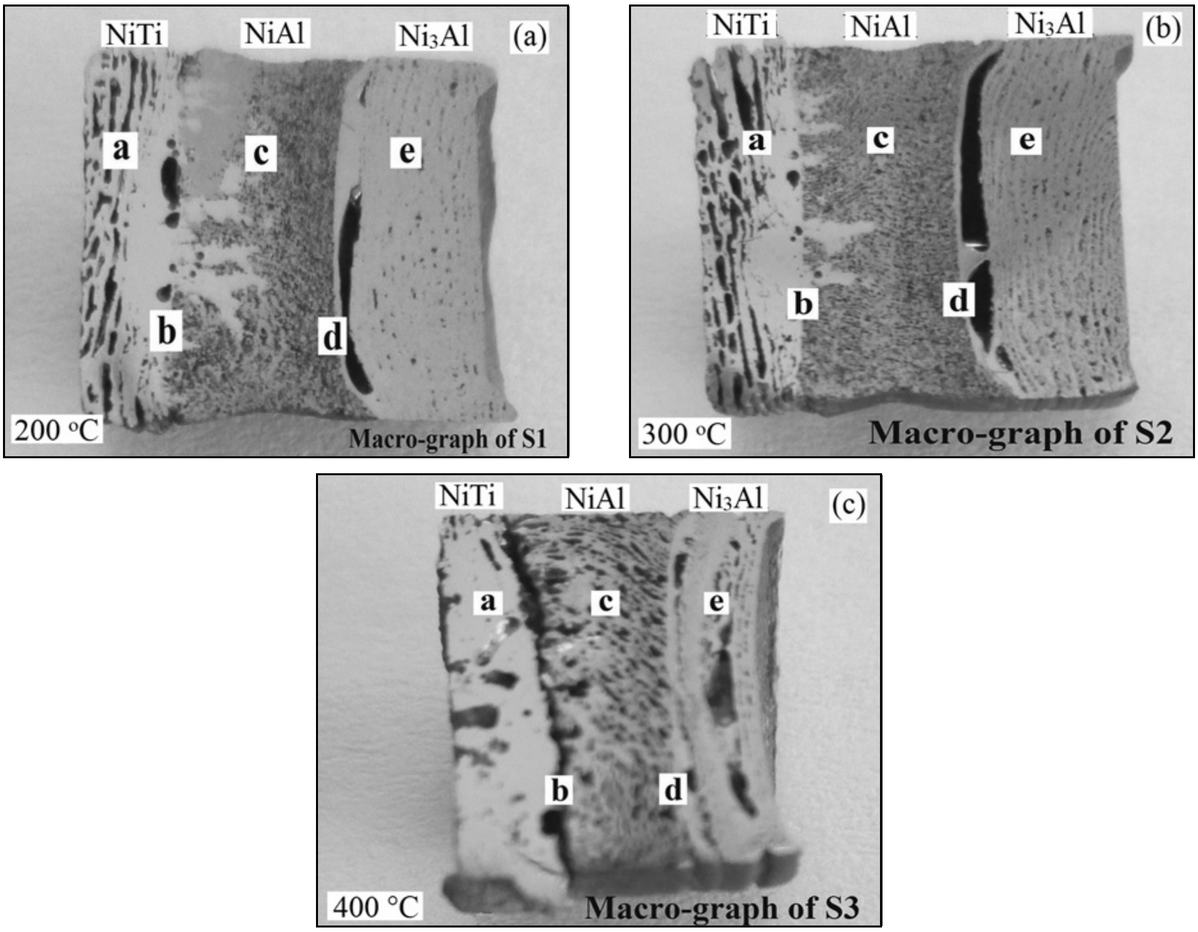

Fig. 2. Macro-surface image of the samples: (a) pre-heat temperature: 200 ℃; (b) pre-heat temperature: 300 ℃; (c) pre-heat temperature: 400 ℃.

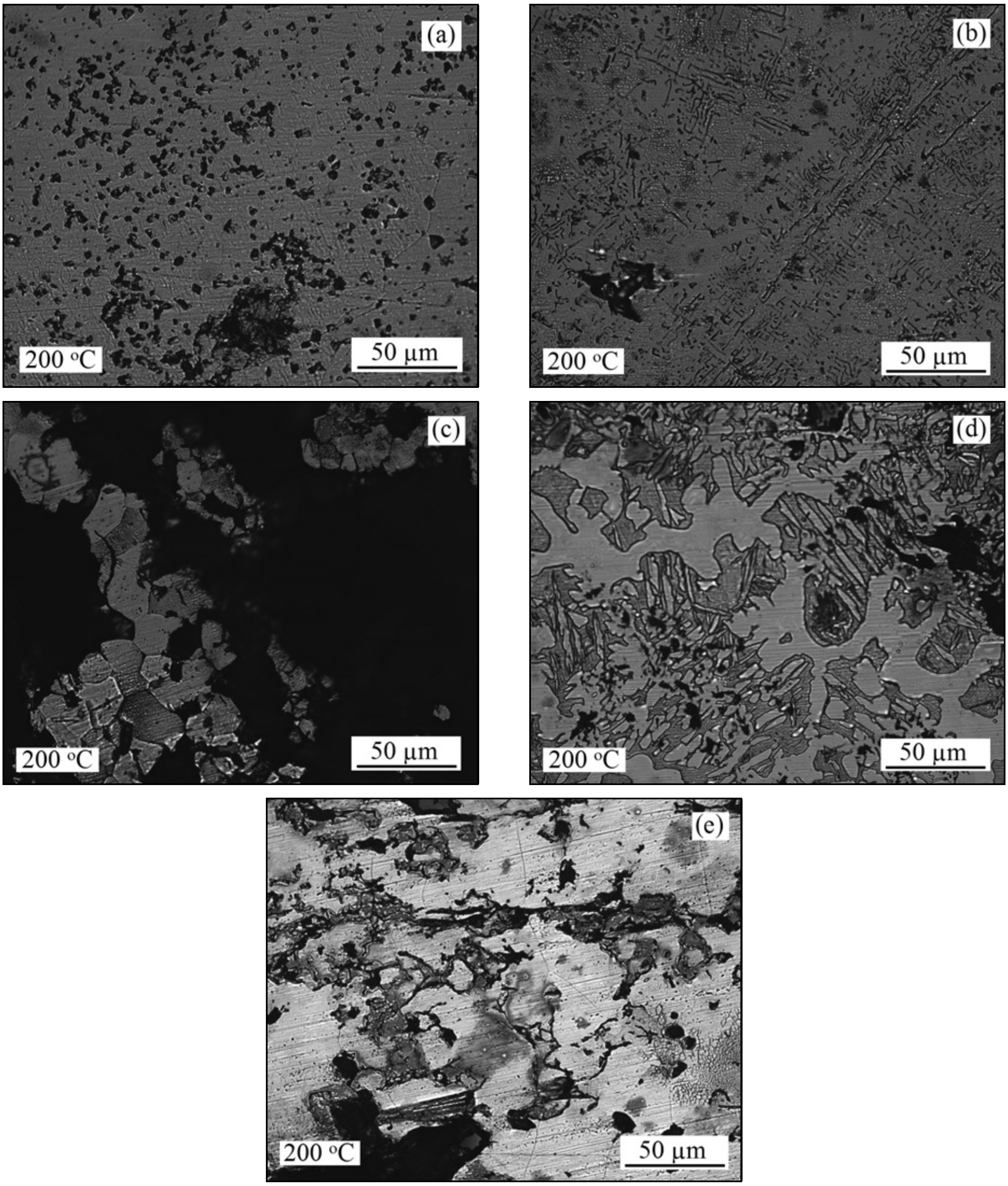

Fig. 3. Optical microscope image of S1 pre-heat temperature: 200 °C.

ages. Also, grains are prominently seen on microstructure images of NiTi, NiAl, and Ni_3Al.

Formation of two types of porosities being external and internal as a result of combustion reaction was assumed. External porosities could be originated from cavities between powders during pre-formation, by vaporization of impurities or gas outlet as the high temperature was reached with the formation of the reaction. Formation of internal porosity may be resulted from the volume difference between reactants and products because the density of products is higher than the density of starting reactants and the product volume is lower than that at the beginning.

3.2. SEM and EDS examination

SEM images and EDS analysis taken from synthesized sample by being pressed under 150 MPa pressure

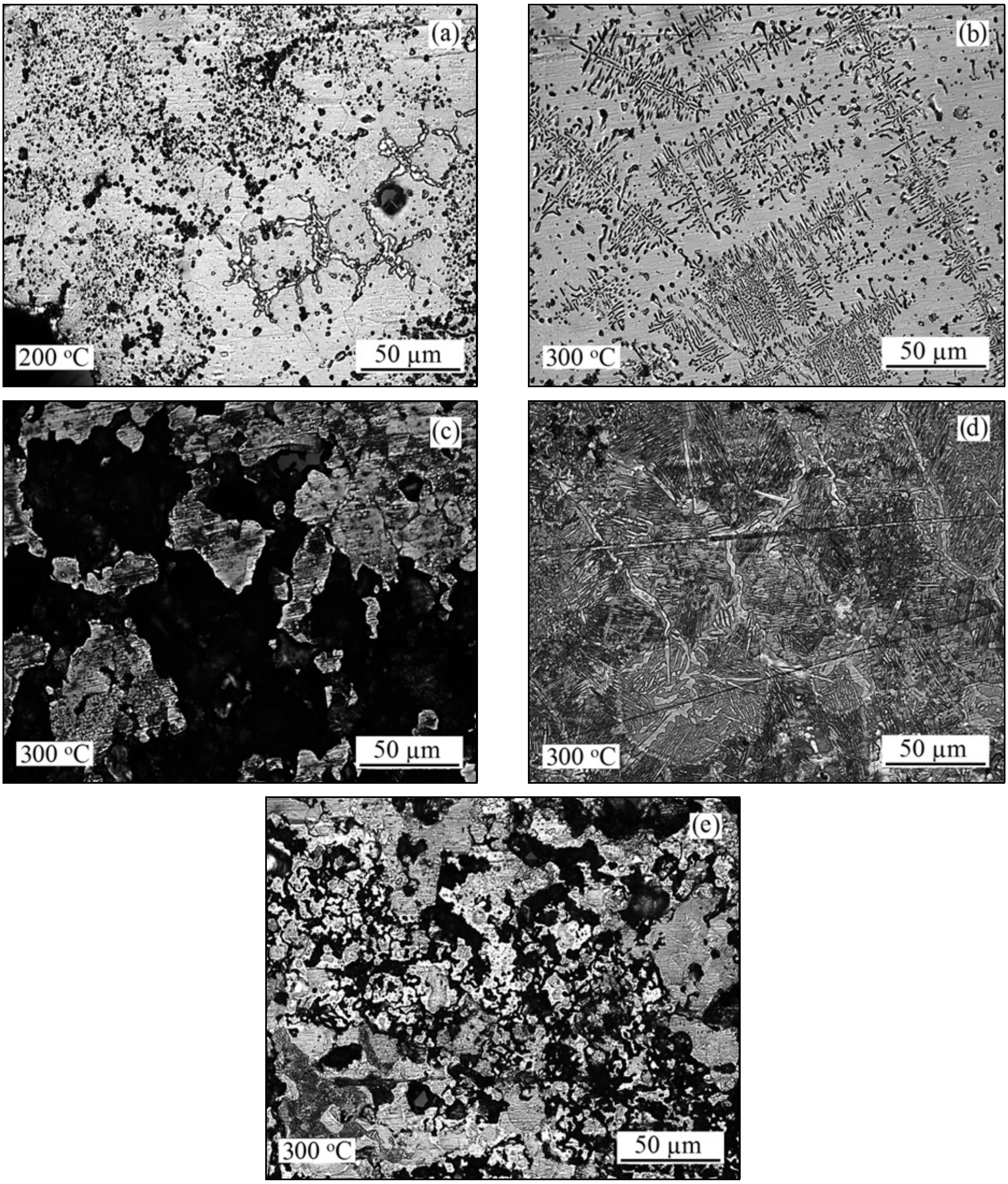

Fig. 4. Optical microscope image of S2 pre-heat temperature: 300 °C.

and using 200, 300, and 400 °C of pre-heating temperatures are shown in Figs. 6a–c and EDS results are shown in Table 2. As a result of EDS analysis taken from intersection of NiTi and NiTi-NiAl, while 41 % Ni and 59 % Ti values were obtained from NiTi side, low amount of Al was obtained along with 47 % Ni and 53 % Ti values from the intersection. When the obtained values were evaluated by the help of Ni-Ti binary equilibrium diagram, it was concluded that the intermetallic phase TiNi + Ti_2Ni in NiTi side and the intermetallic phase TiNi + Ti_2Ni at intersection occurred. The value of 50 % Al and 50 % Ni was obtained in the result of EDS from NiAl side. By the help of Ni-Al binary equilibrium diagram, it was revealed that this phase resulted from AlNi phase. 30 % Al and 70 % Ni values were obtained from the results of EDS taken from Ni_3Al side, and it is concluded that this structure indicated the AlNi + $AlNi_3$ inter-

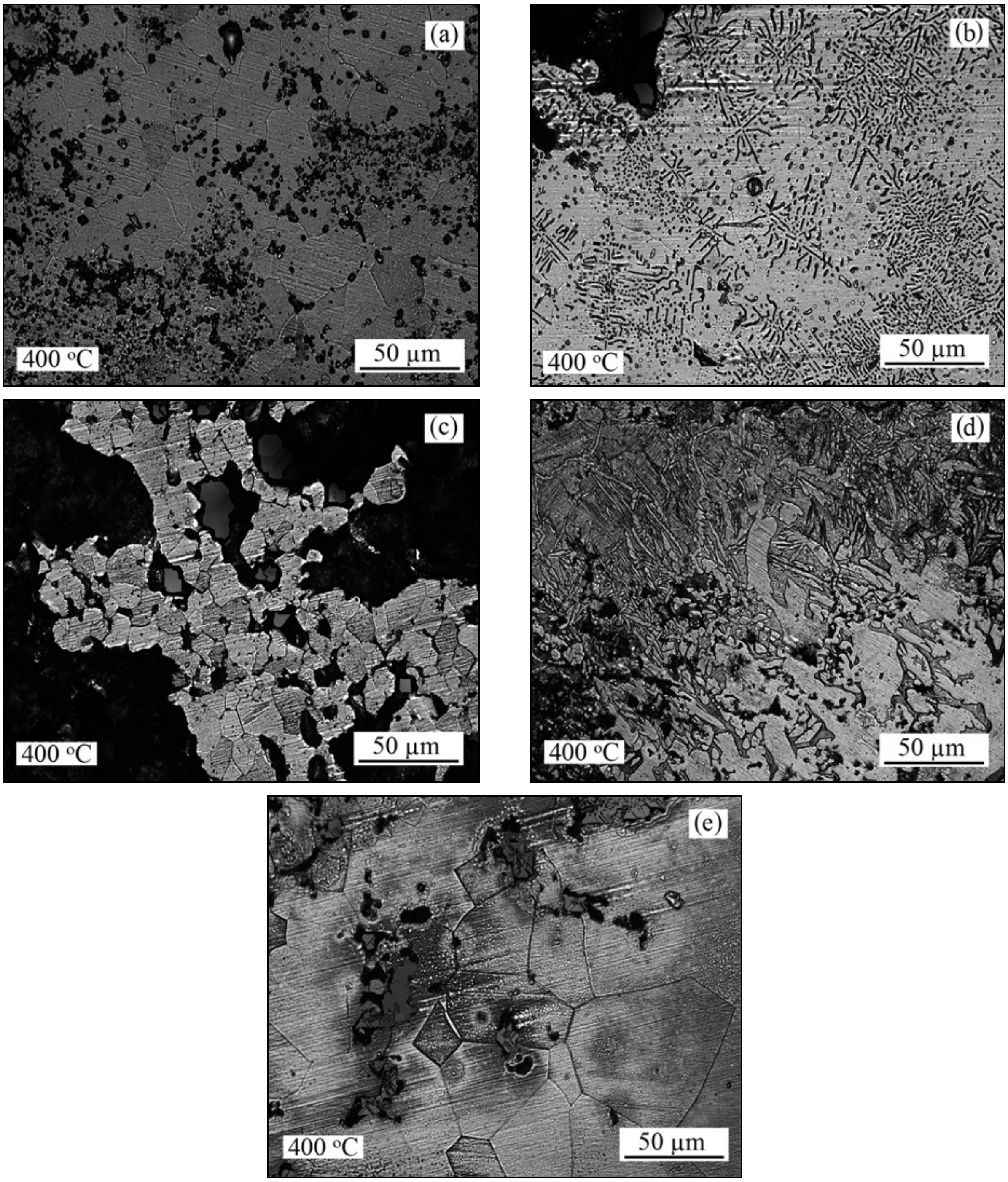

Fig. 5. Optical microscope image of S3 pre-heat temperature: 400 ℃.

metallic phase by the help of Al-Ni binary equilibrium diagram. The results obtained from NiAl-Ni_3Al intersection were 26.76 % Al, and 73.24 % Ni values. It was determined that this value corresponded to Ni_3Al intermetallic phase on Ni-Al binary equilibrium diagram. However, the pores were intense, especially in NiTi site.

Typically, at lower temperatures (< 640 ℃), the SHS reaction of Ni-Al system starts with the formation of Ni_3Al phase, and then Ni_2Al_3 phase is formed. Lastly, NiAl phase occurs. $NiAl_3$ formation reaction is weakly exothermic and a small amount of heat which induce locally the temperature rises remain free [25]. A large amount of the second phase Ti_2Ni was determined as seen in Table 2. As a reactant, with the use of mechanical alloying nanocrystalline Ni-Ti, unreacted Ni phases were eliminated, and secondary intermetallic phase (Ti_2Ni) decreased significantly [26]. Microstructure formed from NiTi and Ti_2Ni phase can be obtained only by heating rapidly ($300\,℃\,min^{-1}$).

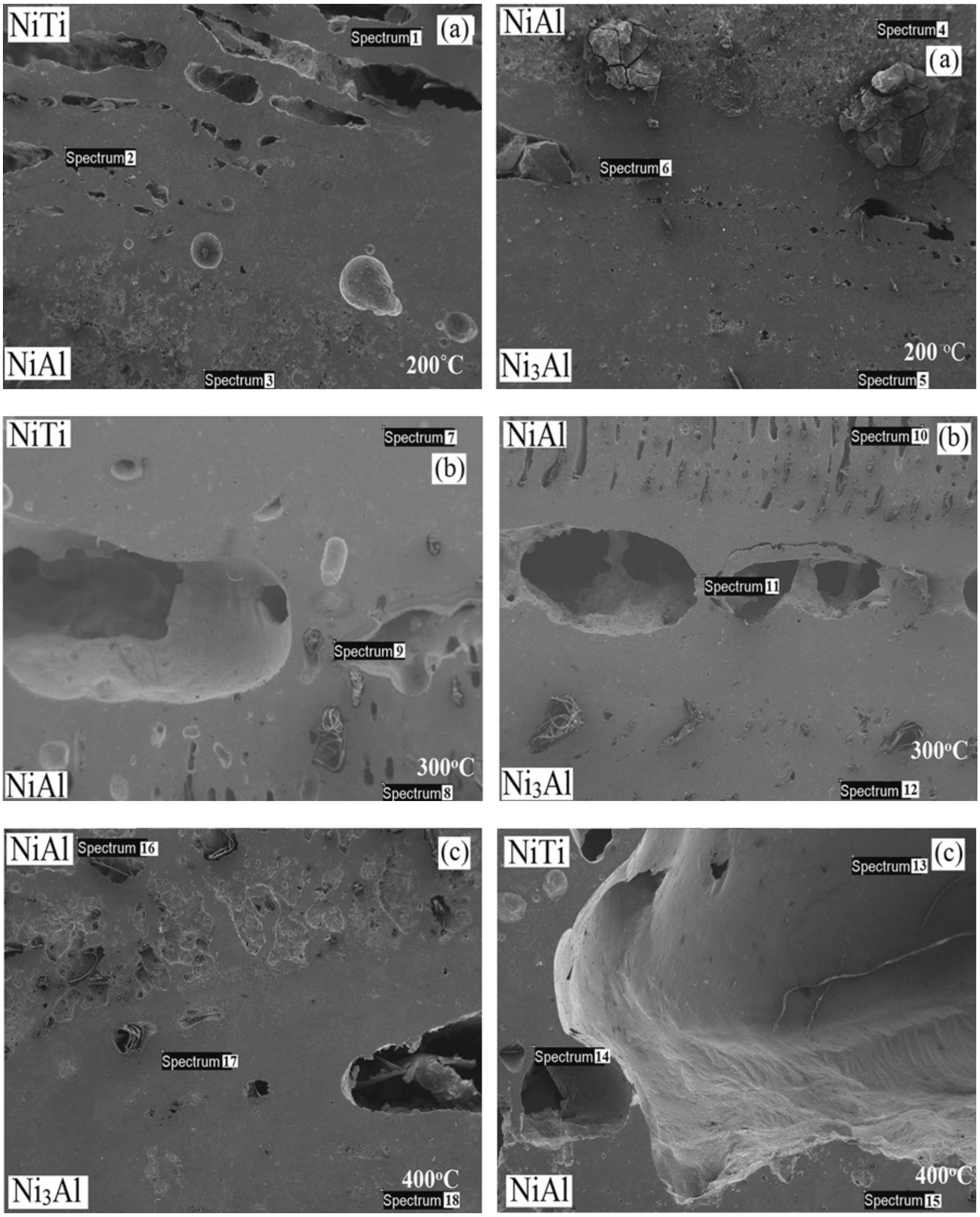

Fig. 6. The SEM micrographs and EDS analyses points of S1, S2, and S3 samples, pre-heat temperatures: (a) 200, (b) 300, and (c) 400 ℃.

Adequate reactive sintering temperature for obtaining NiTi phase is 900 ℃. Further increase in SHS method initial temperature decreases the porosity and the amount of Ti_2Ni phase at 1100 ℃ [27].

NiTi main phase and $NiTi_2$ secondary phase were observed at a low pre-heating temperature (200 ℃). As the pre-heating temperature increased to 300 ℃, NiTi phase formed main structure, and Ni_3Ti_2 phase was seen as the secondary phase. While the pre-heating temperature was increased to 300 ℃, $NiTi_2$ phase with NiTi phase was observed, and Ni_3Ti_2 phase was not observed. Consequently, it is inevitable to obtain some amount of undesirable phase in porous product [28]. In their study, Biswas et al. expressed that multi-phase products at heating rates almost up to 35 ℃ min^{-1} and Al_3Ni,

Table 2. EDS analyses of S1, S2, and S3

Preheat. temperature	EDS point	Element	Mass%	Atomic%	Phase
S1 (200 °C)	Spectrum 1	Ti K	54.00	59.00	TiNi + Ti_2Ni
		Ni K	46.00	41.00	
		Totals	100.00		
	Spectrum 2	Al K	9.66	17.97	τ_4+ Ni_3Ti
		Ti K	25.03	26.22	
		Ni K	65.31	55.82	
		Totals	100.00		
	Spectrum 3	Ti K	47.85	52.94	TiNi
		Ni K	52.15	47.06	
		Totals	100.00	100.00	
	Spectrum 4	Al K	29.18	50.35	AlNi
		Ni K	70.82	49.65	
		Totals	100.00	100.00	
	Spectrum 5	Al K	20.33	30.14	AlNi + Ni_3Al
		Ni K	79.67	69.86	
		Totals	100.00	100.00	
	Spectrum 6	Al K	23.15	26.76	Ni_3Al
		Ni K	76.85	73.24	
		Totals	100.00	100.00	
S2 (300 °C)	Spectrum 7	Ti K	41.52	46.53	TiNi + $TiNi_3$
		Ni K	58.48	53.47	
		Totals	100.00		
	Spectrum 8	Al K	46.05	46.98	NiAl
		Ti K	6.85	7.45	
		Ni K	47.10	45.57	
		Totals	100.00		
	Spectrum 9	Al K	2.16	4.24	TiNi + $TiNi_3$
		Ti K	37.72	41.63	
		Ni K	60.12	54.14	
		Totals	100.00		
	Spectrum 10	Al K	36.95	56.05	AlNi
		Ni K	63.05	43.95	
		Totals	100.00		
	Spectrum 11	Al K	25.59	28.76	NiAl + Ni_3Al
		Ni K	74.41	71.24	
		Totals	100.00	100.00	
	Spectrum 12	Al K	11.87	22.67	Ni_3Al
		Ni K	88.13	77.33	
		Totals	100.00		
S3 (400 °C)	Spectrum 13	Al K	32.05	50.65	AlNi
		Ni K	67.95	49.35	
		Totals	100.00		
	Spectrum 14	Ti K	41.60	46.61	TiNi
		Ni K	58.40	53.39	
		Totals	100.00		

Table 2. (continued)

Preheat. temperature	EDS point	Element	Mass%	Atomic%	Phase
S3 (400 ℃)	Spectrum 15	Al K	2.32	4.47	TiNi + Ti_2Ni
		Ti K	45.84	49.69	
		Ni K	51.84	45.85	
		Totals	100.00		
	Spectrum 16	Al K	28.12	45.98	AlNi
		Ni K	71.88	54.02	
		Totals	100.00		
	Spectrum 17	Al K	12.71	24.06	Ni_3Al
		Ni K	87.29	75.94	
		Totals	100.00		
	Spectrum 18	Al K	27.22	28.11	AlNi + Ni_3Al
		Ni K	72.78	71.89	
		Totals	100.00	100.00	

Al_3Ni_2, NiAl, and non-reacted Ni phases formed [29].

4. Conclusions

1. Functionally graded NiTi/NiAl/Ni_3Al intermetallic compound synthesized by using Ni-Ti-Al powders and self-propagating high-temperature synthesis method was joined successfully.

2. From macro-photographs of samples synthesized by using different pre-heating temperatures, it is seen that especially the NiTi-NiAl zone of samples joined using 200 and 300 ℃ pre-heating temperatures was completely joined, combustion halls formed in NiAl-Ni_3Al zone. It was determined that the sample with 400 ℃ of pre-heating temperature was completely joined from NiAl-Ni_3Al site with the effect of high pre-heating temperature.

3. Formation of dendrites in NiTi-NiAl zone was determined from optical microscopy analyses of samples at all three pre-heating temperatures.

4. Formation of interphases was found with main phases NiAl, Ni_3Al, and NiTi in the examinations of SEM and EDS analysis of samples.

Acknowledgements

We would like to thank the Firat University Scientific Research Projects Coordination for its financial support, Project No. TEKF13.02, and Prof. Dr. Nuri Orhan for his technical assistance.

References

[1] Gao, W. J., Wang, Y. C.: J. Heat Transfer, *123*, 2001, p. 368. doi:10.1115/1.1339976

[2] Bayat, M., Sahari, B. B., Saleem, M.: Int. J. Comput. Methods, *9*, 2012, p. 1240029. doi:10.1142/S0219876212400294

[3] Shah, K., Haq, U. I., Khan, A., Shah, A. S., Khan, M., Pinkerton, J. A.: Mater. Design, *54*, 2014, p. 531. doi:10.1016/j.matdes.2013.08.079

[4] Liang, X., Kou, H., Wang, L., Palmer, C. A., Wang, Z., Liu, G.: Compos. Struct., *132*, 2015, p. 584. doi:10.1016/j.compstruct.2015.05.066

[5] Belabed, Z., Houari, A. S. M., Tounsi, A., Mahmoud, R. S., Bég, A. O.: Compos. Part B, *60*, 2014, p. 274. doi:10.1016/j.compositesb.2013.12.057

[6] Miteva, A. M.: Machines Technologies Materials, *3*, 2014, p. 13.

[7] Aysha C. P. M., S., Varghese, B., Baby, A.: Int. J. Eng. Sci., *3*, 2014, p. 90.

[8] Bharti, I., Gupta, N., Gupta, K. M.: Int. J. Mater. Mech. Manuf., *1*, 2013, p. 221. doi:10.7763/IJMMM.2013.V1.47

[9] Ziegler, T., Kraft, T.: Comp. Mater. Sci., *86*, 2014, p. 88. doi:10.1016/j.commatsci.2014.01.032

[10] Czubarow, P., Seyferth, D.: J. Mater. Sci., *32*, 1997, p. 2121. doi:10.1023/A:1018583024199

[11] Ye, X., Kuang, J., Li, X., Tang, G.: J. Alloy Compd., *599*, 2014, p. 1. doi:10.1016/j.jallcom.2014.02.055

[12] Zhang, X. H., Han, J. C., Du, S. Y., Wood, J. V.: J. Mater. Sci., *35*, 2000, p. 1925. doi:10.1023/A:1004714402128

[13] Makino, A.: Prog. Energy Combust. Sci., *27*, 2001, p. 1. doi:10.1016/S0360-1285(00)00004-6

[14] Çirakoğlu, M., Bhaduri, S., Bhaduri, B. S.: J. Alloy Compd., *347*, 2002, p. 259. doi:10.1016/S0925-8388(02)00499-1

[15] Sofiyev, H. A., Kuruoglu, N.: Compos. Part B, *45*, 2013, p. 1133. doi:10.1016/j.compositesb.2012.09.046

[16] Sadollah, A., Bahreininejad, A.: J. Mech. Behav. Biomed. Mater., *4*, 2011, p. 1384.

doi:10.1016/j.jmbbm.2011.05.009

[17] Kiani, K.: Compos. Struct., *107*, 2014, p. 610. doi:10.1016/j.compstruct.2013.07.035

[18] Stoloff, N. S.: Metallurgical Trans. A, *24*, 1993, p. 561. doi: 10.1007/BF02656626

[19] Cinca, N., Lima, C. R. C., Guilemany, M. J.: J. Mater. Res. Technol., *2*, 2013, p. 75. doi:10.1016/j.jmrt.2013.03.013

[20] Kopit, Y.: Intermetallics, *9*, 2001, p. 387. doi:10.1016/S0966-9795(01)00013-9

[21] Chen, S. P., Meng, Q. S., Zhao, J. F., Munir, Z. A.: J. Alloy Compd., *476*, 2009, p. 889. doi:10.1016/j.jallcom.2008.09.162

[22] Kumar, K. G., Sivarao, T., Anand, J. S.: Int. J. Eng. Techn., *11*, 2011, p. 208.

[23] Burkes, E. D., Moore, J. J.: J. Eng. Mater. Technol., *128*, 2006, p. 445. doi:10.1115/1.2204950

[24] Kiliç, M., Kirik, I., Kurt, B., Orhan, N.: In: Proc. of the 15th International Materials Symposium IMSP'2014. Ed.: Meran, C., Denizli, Pamukkale University 2014, p. 488.

[25] Dong, S., Hou, P., Yang, H., Zou, G.: Intermetallics, *10*, 2002, p. 217. doi:10.1016/S0966-9795(01)00109-1

[26] Goh, W. C., Gu, W. Y., Lim, S. C., Tay, B. Y.: Intermetallics, *15*, 2007, p. 461. doi:10.1016/S0966-9795(01)00109-1

[27] Novák, P., Mejzlíková, L., Michalcová, A., Čapek, J., Beran, P., Vojtěch, D.: Intermetallics, *42*, 2013, p. 85. doi:10.1016/j.intermet.2013.05.015

[28] Tosun, G.: Production of a Ni-Ti Alloy Implant and Investigation of its Biocompatibility in Vivo. [Ph.D. Thesis]. Elazig, Institute of Natural Sciences, Firat University 2007.

[29] Biswas, A., Roy, S. K., Gurumurthy, K. R., Prabhu, N., Banerjee, S.: Acta Materialia, *50*, 2002, p. 757. doi:10.1016/S1359-6454(01)00387-1